

The State of the Loop Model

2002

Rebecca McMullen

February 8, 2006

1 Introduction

Above the sun's surface the temperature rises rapidly from 5,000 K to 2,000,000 K in the corona. How the sun maintains this steep temperature gradient despite constant radiative losses is unknown, and one of the great problems of coronal studies. Observations tell us the Corona is made of strong magnetic fields and ionized gas, predominately hydrogen, which appears to be organized in loop structures. Transient heating events of various time scales seem to occur in these loops triggering large flares, as well as smaller scale events. Understanding the energetics of a single loop may bring us a long way toward understanding the entire Corona.

The dynamics of the corona are governed by the Magnetohydrodynamic (MHD) equations, a set complex set of coupled partial differential equations derived from conservation of mass, momentum, energy, Maxwell's Equations and Ohms law.

$$\begin{aligned}\frac{\partial \rho}{\partial t} + \nabla \cdot (\rho \mathbf{v}) &= 0 \\ \frac{\partial \mathbf{v}}{\partial t} + (\mathbf{v} \cdot \nabla) \mathbf{v} &= \mathbf{F} - \frac{1}{\rho} \nabla P + \frac{1}{4\pi\rho} (\nabla \times \mathbf{B}) \times \mathbf{B} + \frac{1}{\rho} \nabla \cdot (\mu \nabla \cdot \mathbf{v}) \\ \frac{\partial \varepsilon}{\partial t} + \nabla \cdot (\varepsilon \mathbf{v}) &= -P \nabla \cdot \mathbf{v} + \nabla \cdot (\kappa \nabla T) - n_e^2 \Lambda(T) + E_H + \mu (\nabla \cdot \mathbf{v})^2 \\ \frac{\partial \mathbf{B}}{\partial t} &= \nabla \times (\mathbf{v} \times \mathbf{B}) + \lambda \nabla^2 \mathbf{B}\end{aligned}\tag{1}$$

Although analytic solutions to the MHD equations do exist for specified geometries, solving this set of equations for a specific set of initial conditions in the domain of the corona from the Transition Region out to about $10R_\odot$ is generally considered an intractable problem.

The problem is simplified considerably by the basic assumption $\lambda = 0$, which together with Kelvin's Theorem restricts plasma to move only along the field lines. This ideal limit of MHD is valid for velocities well below the Alfvén speed, and allows us to make progress. Assuming that in the time period considered the magnetic field is reasonably static, we can study the dynamics of a single coronal loop as it is heated and cooled in the sun's atmosphere. The passive magnetic field is removed from the equations, which simplify to the Hydrodynamic Equations. These equations may be solved numerically.

Variable	x	$lhist.e$	$lhist.n_e$	$lhist.v$	q_0	g	a
Elements	N-1	N	N	N	N-2	N-1	N-1

Table 1: Elements required in the numerical model for staggered grid variables.

In this paper we will outline one hydrodynamic loop model, discussing the specifics of the Numerical Model developed between 1998 and 2002 at Montana State university by Charles Kankelborg, Rebecca McMullen, and Dana Longcope. Section 2 will discuss specifics to the model and testing methods used. Section 3 looks at practicalities, where the codes can be found and what initial conditions may be given the code. Section 4 shows an example run from an initial state to an equilibrium state. Section 5 shows an example of heating a coronal loop and discusses problems with the grid. Section 6 simulates various TRACE responses to the model, for comparison with real data.

2 Numerical Model

Assuming ideal plasma and applying the restrictions of a single loop geometry, the MHD Equations of 1 may be restated in a simplified Hydrodynamic form. Equations 2 assume that x , the loop coordinate, A , the cross sectional area, and g_{\parallel} , the component of gravity along the magnetic field, together specify the three dimensional geometry of a coronal loop of arbitrary shape.

$$\begin{aligned}
\frac{\partial n_e}{\partial t} &= -\frac{1}{A} \frac{\partial}{\partial x} (A n_e v) \\
\frac{\partial v}{\partial t} &= -\frac{1}{n_e m_p} \frac{\partial P}{\partial x} + g_{\parallel} - v \frac{\partial v}{\partial x} + \frac{1}{n_e m_p A} \frac{\partial}{\partial x} \left(\mu \frac{\partial}{\partial x} A v \right) \\
\frac{\partial \varepsilon}{\partial t} &= -\frac{1}{A} \frac{\partial}{\partial x} (A \varepsilon v) - \frac{P}{A} \frac{\partial}{\partial x} (A v) + \frac{1}{A} \frac{\partial}{\partial x} \left(A \kappa_0 T^{5/2} \frac{\partial T}{\partial x} \right) - n_e^2 \Lambda(T) + E_H + \mu \left(\frac{1}{A} \frac{\partial}{\partial x} A v \right)^2
\end{aligned} \tag{2}$$

These equations, along with the equations of state, $P = (2/3)\varepsilon = 2n_e k_B T$, govern the coronal dynamics of the flux tube. In the above equations, P is pressure, T is temperature, n_e is electron density, ε is the energy density, v is the bulk velocity, and E_H is a user specified volumetric heating function. Collisional effects enter in the variables representing conduction κ , kinematic viscosity $\nu = \mu/m_p n_e$, and radiative losses Λ . The state of the loop is fully specified by the variables $n_e(x, t)$, $v(x, t)$, and $\varepsilon(x, t)$.

The state variables n_e , v , and ε are defined on a staggered grid, with array elements as listed in Table 1. The staggered grid defines quantities in an intuitive manner, such that the energy density ε_i belongs to a volume between two grid points, at x_{i-1} and x_i . Similarly, the velocities are defined at the boundaries of that volume, so that v_i is associated with the surface with area A_i at the position x_i . This makes upwind differencing a first order calculation. To keep track of which array has how many elements, the user should use the program `sizecheck.pro`, which may be called `IDL>sizecheck, lhist,g,A,x, E_h`, and will stop and print an error message if any array has the wrong number of elements.

The code `loop1003.pro` takes the current state variables as input, and solves the equations in 2 for the state variables projected ahead in time a time step Δt with typical values of 1 or 5 seconds. It uses x , A , g_{\parallel} , E_H as additional input, but assumes that these remain constant for the time step Δt . The Magnetic field does not enter explicitly into this calculation.

The time stepper `loop1003` evolves the state variables Δt in time, by taking numerous smaller steps dt at the Courant limit. It uses a second order Runge-Kutta Midpoint type method, with the initial midpoint time step increased from $0.5 dt$ to $0.6 dt$ for stability. The terms of the HD equations in 2 are handled separately through operator splitting, such that the bulk of the terms are calculated by first order explicit differencing. The derivatives in the viscous and conductive terms are calculated by implicit differencing, necessitating matrix transformations, but allowing the time steps dt to be longer. A more thorough explanation of this phenomena may be found in the term paper `math567paper.ps` written on viscosity for Physics 567.

To simulate a longer period of time, the routine `evolve10.pro` may be employed, for which `loop1003.pro` is a sub routine. The state variables are concatenated at time resolution ΔT to a loop history structure `lhist` after each return of the sub-routine. `evolve10.pro` has several built in checks, as well as the ability to allow the user to monitor progress by setting the `showme` keyword. A demonstration of this is discussed in Section 4.

The length of the time steps dt taken by the time stepper are determined by the Courant Condition for stability. As information propagates between cells of the grid, the Courant Condition acts to increase dt such that one side of the cell always knows what the other is doing. Mathematically this may be written

$$\Delta t \leq \frac{\Delta x}{|v|}$$

Thus a shock propagating through the grid with speed v will not move into an adjoining cell before the calculation finishes. Practically speaking, the effect is to force the code to take smaller time steps when the resolution is high (small Δx) or velocity is high, as in the transition region. Small time steps mean more computation time and a high overall run time for the code.

Although a significant fraction of the plasma in the real Corona is not hydrogen, the model used only hydrogen for the bulk calculations. Collisional effects from ions are still of large importance to the model, especially in matters of heat transfer. It was never the desire of those who developed this code to treat atomic physics any more thoroughly than the minimal sufficiency possible. The aim of the study has always been the bulk effects where possible, but the importance of atomic physics to energy transfer demands that we take it into account.

The code uses tables to look up the values for radiation and conduction as functions of the temperature, interpolating between the table values. The values used are a matter of much debate in Solar Physics, so choices are provided. Figure 1 shows conduction values suggested by Vesecky et al. (1979), as well as the code default recommended by Kankelborg, which includes an bipolar diffusion modifications to the H $L\alpha$ peak (Avrett, 1991) and enhanced losses due to the FIP effect (Martens, Kankelborg and Berger, 1999). Spitzer's conductivity calculation of 1962 has long been the standard and is offered as an option, but suspected

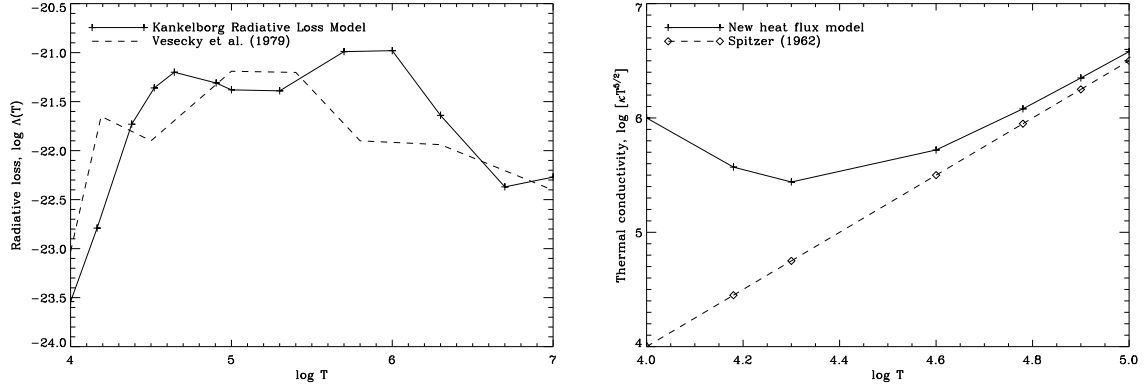


Figure 1: Lookup tables for $\Lambda(T)$, $\kappa_0(T) T^{5/2}$. The linear decrease to zero for Radiative losses with $9500K \leq T \leq 40000K$ cannot be shown on a log plot. The Kankelborg Model for Conductivity κ_0 has discontinuities outside of the plot range.

diffusion of protons and neutral hydrogen in regions of steep temperature gradient caused us to use a new model, which is the solid line in Figure 1.

Viscosity is calculated as a function of temperature, from the Plasma Formulary [4]

$$\nu_{\parallel}^p = \frac{\mu_{\parallel}^p}{m_p n_e} = 0.96 \frac{(k_B T_p)^{5/2}}{m_p n_e} \frac{3\sqrt{m_p}}{4\sqrt{\pi} e^4 \lambda} \quad [4]$$

This model has been tested extensively by comparison to analytical solutions by C. Kankelborg and in the math paper `math567paper.ps`, but has not been tested after the most recent modifications. Such testing, however, requires extensive modifications to the code, as analytical solutions are typically un-physical. Testers often wonder just what code is being tested by such methods.

Another useful exercise is to compare the output of two numerical codes developed by different research groups. In this spirit, James Klimchuk of the NRL has generously donated some loop models which can be found in `/mcmullen/bp_sim/klimchuk/loop_0.sav`. Unfortunately, it is often difficult to resolving the differences between solutions found by two separate codes.

3 Sample Initial State

In the course of normal use, most input data comes from potential field extrapolations from real images, the latest of which is `xbp1_1020.sav`. This extrapolation comes from an X-ray Bright Point observed at 10:20 UT on 17 June 1998 by TRACE, and referred to as XBP1. We will not discuss here how such extrapolations are generated or the selection criteria for data sets. Instead we focus on generating an initial state acceptable to the numerical model.

A new loop geometry usually requires a specific script, frequently modified from an old one. The most recent of these scripts is `start_xbp1.pro`, which was written specifically for the `sav` file mentioned before. It reads in the file which contains a three dimensional loop axis, one dimensional

Path from /home/mcmullen/	File Name	Contents
/bp_sim/charles/	loop1003.pro bnh_splint.c stateplot.pro	MSU Loop Model, time stepper Interpolation sub-routine Displays state variables
/bp_sim/myprogs/	evolve10.pro hd_terms.pro regrid4.pro start_xbp1.pro nanoflare1.pro sizecheck.pro ltrace.pro	Drives time stepper loop1003.pro Displays terms of the HD equations Moves grid to minimize temperature gradient Initializes loop from xbp1_1020.sav Adds TRACE light curves, mimics nanoflare event Checks for sufficient Chromosphere depth Generates TRACE light curve for loop model
/bp_sim/klimchuk/	loop_0-2000.sav start_NRLtest1.pro do_NRLtest1.pro	Klimchuk Loop Model for $t = 0 - 2000s$ Initiates MSU model similar to Klimchuk Heats MSU model to Klimchuk specifications
/bp_sim/data/new_xbp1/	xbp1_*.sav xbp1eq2_*.sav	XBP1 grid 1 save files XBP1 grid 2 save files
/bp_sim/dana/	xbp1_1020.jpg xbp1_1020.sav	MDI Image of XBP1, extrapolation overlayed Save file of XBP1 extrapolation
/bp_sim/writeup/	paper.ps agu0601poster.ps agu1201poster.ps y10poster.ps y10paper.ps spd0602poster.ps math442paper.ps math567paper.ps	This research summary Poster presented at AGU June 2001 Poster presented at AGU December 2001 Poster presented at Yohkoh Meeting January 2002 Paper in Yohkoh Proceedings Poster presented at SPD June 2002 Paper on wave heating, MA442 Paper on viscosity, PH567

Table 2: Locations and contents of important files.

arrays of loop coordinate, crosssectional radius, field strength and gravitational component as a function of the loop coordinate. It generates an estimated equilibrium state based on the scaling laws of Rosner, Tucker and Vaiana, 1978 [9] for uniformly heated ($q_0 = E_H = \text{const.}$) semi-circular loops of half-length L .

$$T_{max} = 1.4 \cdot 10^3 \left(\frac{q_0 L^2}{9.8 \cdot 10^4} \right)^{2.7} \quad (3)$$

$$P = \left(\frac{T_{max}}{1.4 \cdot 10^3} \right)^3 \frac{1}{L} \quad (4)$$

The initiation script also uses an empirical fit to the incomplete-beta function to calculate temperature.

$$T(x) = T_{max} \left(4 \frac{x}{2L} \left(1 - \frac{x}{2L} \right) \right)^{0.333333} \quad (5)$$

These equations are combined with equations of state, to calculate the state variables n_e , and ε as functions of the position variable x . The state variable v is left at zero initially, and no coronal temperatures are initially allowed below $10^4 K$.

$$n_e = \frac{1}{2} \frac{P}{k_B T} \quad (6)$$

$$\varepsilon = \frac{3}{2} \cdot 2 n_e k_B T \quad (7)$$

The energetics of the Corona are intimately linked with those of the Chromosphere by virtue of heat conduction at the Transition Region interface. Bulk flows of matter along the magnetic field lines connecting the Corona and Chromosphere can also be of high amplitude when evaporation or condensation is energetically favorable. We cannot, therefore, exclude a model of the Chromosphere from our treatment of the Corona.

The Chromosphere acts as a mass and particle reservoir, and for our purposes is modeled as a gravitationally stratified atmosphere of constant temperature $T_0 = 10^4$, and depth of at least two scale heights.

$$n_{e \text{ chrom}} = n_{e0} e^{-|g_0| \frac{1}{2} m_p (x_{chrom} - x_0) / (k_B T_0)} \quad (8)$$

$$\varepsilon = \frac{3}{2} \cdot 2 n_{e \text{ chrom}} k_B T_0 \quad (9)$$

The initial state generated by `start_xbp1.pro` can be seen in Figure 2. The pressure plot shows clearly the RTV model with an exponentially stratified Chromosphere tacked on. Figure 2 was generated by the routine `stateplot.pro`.

The high density in the Chromosphere causes massive radiative losses, necessitating increased heating per unit volume to stay at $T_0 = 10^4 K$. In the real sun, radiation from lower levels is absorbed by the Chromosphere, stabilizing the temperature. However, we are not concerned with this interaction. We choose instead to fool the program by artificially lowering the radiative losses at Chromospheric temperatures. The radiative losses decrease linearly between $10^4 K$ and $9500 K$ so that all radiation shuts off if the temperature falls below $9500 K$. Once radiative cooling shuts off, the temperature quickly rises above the $9500 K$ cutoff. This allows the model Chromosphere to be stabilized at $T = T_0$ for the same level of uniform volumetric heating input to the Corona.

While this Chromospheric heating trick is useful, it does somewhat limit the scope of questions that may be studied with this code. Asymmetric heating has been shown to cause condensation in

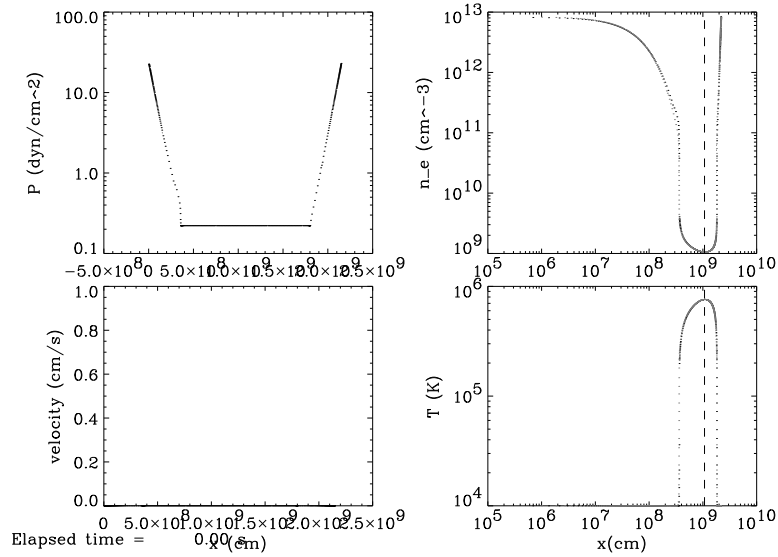


Figure 2: Initial state for XBP1. The state is initiated by application RTV scaling laws with uniform volumetric heating of $7 \cdot 10^4 \text{ erg cm}^{-3} \text{ s}^{-1}$, with an exponential chromosphere attached below the Transition Region.

loop tops or loop legs, a behavior that may be linked to cool prominence observed in the Corona. The Chromospheric heating trick, however, does not allow these condensates to be studied by this code, as the physics of their cooling applied by the code is not real.

4 Sample Loop Equilibrium

The initial state for XBP1 shown in Figure 2 is not an equilibrium state for the Hydrodynamic Equations shown in 2. Even if the geometry were perfectly semi-circular, the patched together Corona and Chromosphere are not quite right for this loop. The initial system is analogous to a rubber band held tight. Starting the time evolution code typically initiates large flows in the loop, as the system relaxes toward equilibrium.

The following commands established near equilibrium for XBP1, generating the files `xbp1_2000.sav`, `xbp1_2000regrid4.sav`, `xbp1_3000.sav`, `xbp1_3000regrid4.sav`, `xbp1_10000.sav`, `xbp1_10000regrid4.sav`, and `xbp1_eq.sav`. The relaxation of the apex and footpoint temperatures as functions of time can be seen in Figure 3, as the loop relaxes from the RTV state toward Hydrodynamic Equilibrium, overshoots, and returns.

```
;-----Initiate Loop
path='~/bp_sim/data/new_xbp1/'
start_xbp1,/newfile, outfile=path+'xbp1_start.sav'

;-----run to equilibrium
evolve10,path+'xbp1_start.sav', 2000., 5., outfile=path+'xbp1_2000.sav',$
    q0=0.0007, showme=1
regrid4, infile=path+'xbp1_2000.sav',/showme
```

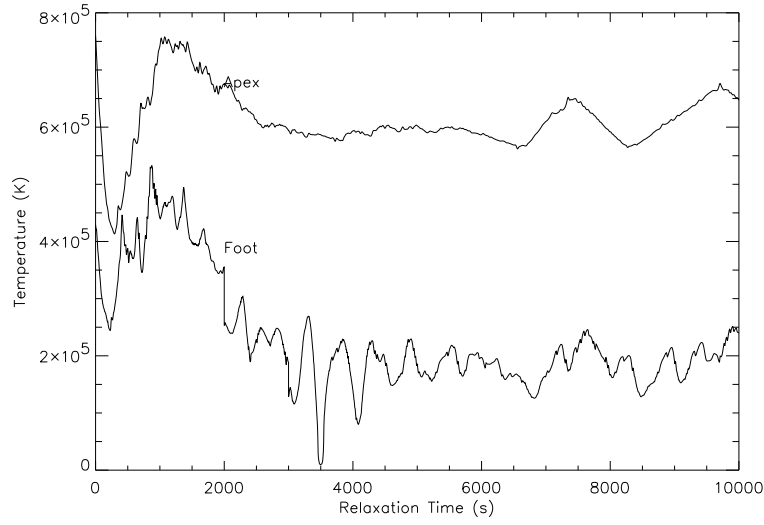


Figure 3: The model begins in an RTV state, and relaxes toward an equilibrium state, where it will satisfy Equations 2, to low order.

```

evolve10,path+'xbp1_2000regrid4.sav', 1000., 5., outfile=path+'xbp1_3000.sav',$
    q0=0.0007, showme=1
regrid4, infile=path+'xbp1_3000.sav',/showme
evolve10,path+'xbp1_3000regrid4.sav', 7000., 5., outfile=path+'xbp1_10000.sav',$
    q0=0.0007, showme=1
regrid4, infile=outfile outfile=path+'xbp1_10000.sav',/showme
evolve10,path+'xbp1_10000regrid4.sav', 100., 5., outfile=path+'xbp1_eq.sav',$
    q0=0.0007, showme=1
END

```

The repeated calls to the function `regrid4.pro` in this script is an attempt to adjust the grid more optimally to the shifting transition region. The initialized state of the loop did refine the Transition Region grid, but as the code adjusts the area in need of resolution tends to drift. `regrid4.pro` attempts to move the high resolution to where it is needed. This routine does not attempt to conserve momentum, energy or mass and therefore ought not be run for any scientific purpose.

Higher versions of `regrid4.pro` are not in running order. Version 4 moves the grid spacing on the existing loop model subject to the conditions that $1/1.5 < \Delta n_{ei}/\Delta n_{ei-1} < 1.5$, the density may change by no fraction greater than 1.5 in a single step. Simultaneously, version 4 imposes the condition that $1/1.5 < \Delta A_i/\Delta A_{i-1} < 1.5$, keeping the loop area from changing too abruptly. Future versions of `regrid.pro` will ideally, attempt to smooth out the spatial step size, making $1/1.5 < \Delta x_i/\Delta x_{i-1} < 1.5$.

Unfortunately, the grid resolution is a pressing problem in the state of this Loop Model. Figure 4 shows two grids for the same XBP1 loop model, with modest differences. Grid 1 was adjusted from an equilibrium state which was then heated to model an impulsive event. Grid 2 was adjusted at the peak of heating, and applied to the equilibrium state of grid 1. That model with grid 2 was then heated at the same rate as that with grid 1. Figure 5 shows the temperature structure of the loop with both grids after 900 seconds of heating. The divergence of the models with microscopic

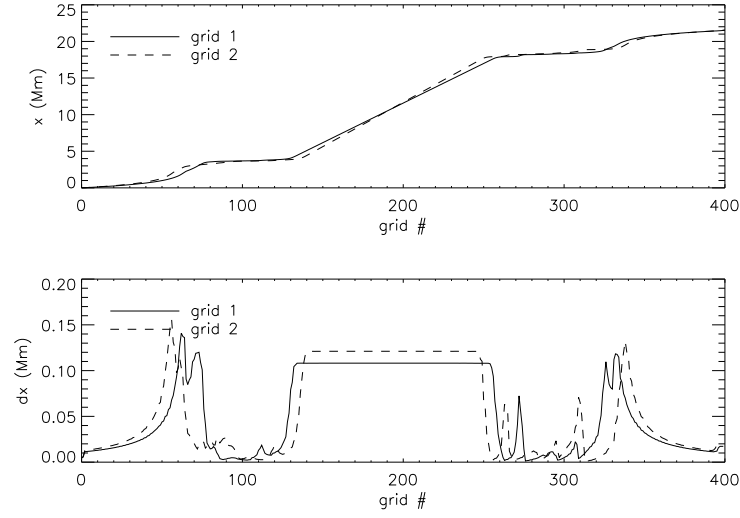


Figure 4: Different grids for XBP1 Loop Model. Discontinuities in dx may cause solutions to diverge.

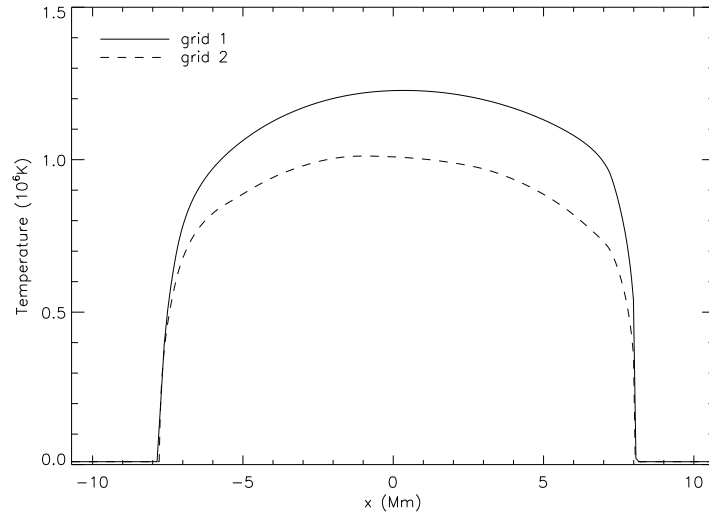


Figure 5: Macroscopic differences in XBP1 temperature models after 900 seconds heating with two different grids resolutions, as in Figure 4

resolution differences is shown to be macroscopic.

This result calls into question the usefulness of the entire Loop Model. If small differences in grid resolution in the Transition Region result in macroscopic differences in loop dynamics, then either the entire loop is not being resolved well enough or there is some chaos in the system. How and to what conditions the grid is to be optimized is a pressing question. Alternately the discontinuities in the derivative of x as shown in Figure 4 may cause large contributions in some terms of the calculation, causing dynamic differences. This question has not been explored. If it cannot be resolved, the development or acquisition of a Loop Model with a self adjusting grid may be necessary.

5 Sample Heated Loop

The equilibrium state achieved in the previous section can be heated to simulate an impulsive flare. The same code can be run with the **energy** keyword set to the value of total energy deposited, in the time t_0 . The energy is divided up in a sub-routine of **evolve10.pro** among the corona grid cells as defined by the two dimensional array **n_depth**, such that the heat density is constant through the loop. The loop is then allowed to relax back to equilibrium while the original background heating is applied. The following commands generated the file **xbp1_2.3e25_2000.sav**.

```
;-----set the time back
restore,outfile=path+'xbp1_eq.sav'
lhist.time=lhist.time-max(lhist.time)
save, filename=path+'xbp1_eq.sav', lhist,g,A,x, E_h, delta_t, orig, n_depth, note

;-----heat with total energy 2.3e25 erg
energy = 2.3e25 ;erg
q0 = 0.0007 ;erg/s/cm^3
t0 = 1000. ;s
infile = path + 'xbp1_eq.sav'
outfile= path + 'xbp1_2.3e25.sav'
dt = 5.
evolve10, infile, t0, dt, outfile=outfile, energy=energy,bgheat=q0, $
    showme=1, computer='mithra'

;-----cool down
q0 = 0.0007
t0 = 2000.
infile = path + 'xbp1_2.3e25.sav'
outfile= path + 'xbp1_2.3e25_2000.sav'
dt = 5.
evolve10, infile, t0, dt, outfile=outfile, q0=q0, $
    showme=1, computer='mithra'
END
```

The apex temperature response to these commands is shown in Figure 6. Once heating turns off, the loop over compensates and cools too much. Application of the original background heating returns the loop to its equilibrium state after about 3000s.

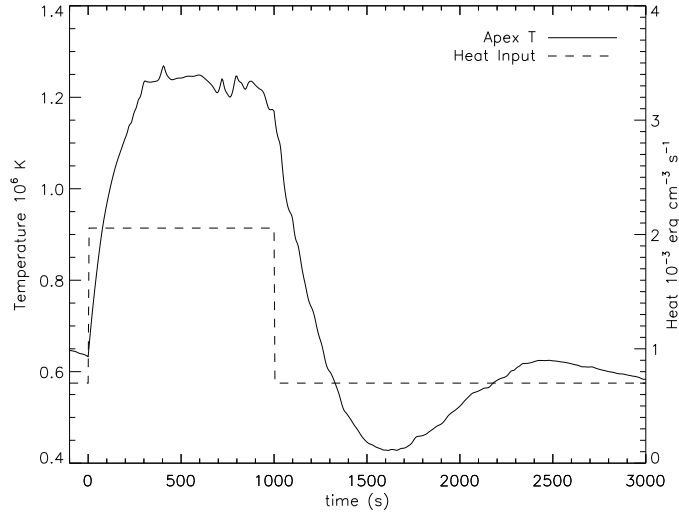


Figure 6: Loop top temperature response to heating function for model XBP1.

The keyword `computer` is used in this example to specify which set of compiled object code to access. The `c` sub-routines have been compiled for `Mithra` and `Earth`, and the compiled object code is located in separate directories, where the code runs. Currently the only choices allowed for this keyword are `Mithra` and `Earth`, with `Earth` set as default.

Figure 7 shows Frame 200 at $t = 950$ from a movie of XBP1's divergent evolution on grids 1 and 2. The entire movie can be seen in `/mcmullen/bp_sim/plots/gridmovie2.mpg`. The movie compares the same loop model evolving on two different grids.

Turning on heating as a step function in time has generally proven problematic by generating shocks which increase without bound. For some reason, the loop model XBP1 in files `xbp1_2.3e25_2000.sav` and `xbp1eq2_2.3e25_2000.sav` managed to escape. Typically, the shocks generated at heating onset increase in amplitude without bound until the calculation of the time step crashes the computer

$$\Delta t \leq \frac{\Delta x}{|v|}$$

by returning the value $\Delta t = -NaN$. We speculate that the increasing flux tube area, where the magnetic field opens out from the Chromosphere into the Corona causes a bulk acceleration, enhancing the velocity as particles flow up from the Chromosphere. Alternately, the shock and velocity increase may be related to a lack of grid resolution in the transition region. These questions, and the reason this problem did not occur in the sample given here, are unanswered.

6 Analysis

To compare the model to the original data, one can simulate an instrument response to the model. The TRACE responses shown in Figures 8 and nano were generated from the Loop Model XBP1 in the file `/xbp1_2.3e25_2000.sav` by the procedure in the program `/writeup/plots3.pro`.

One key routine used in this procedure is `ltrace.pro`, which generates a TRACE passband-specific response to the loop model. To attain a realistic value, the massive emission generated by the artificial Chromosphere must be blocked by trimming the arrays before they are input to

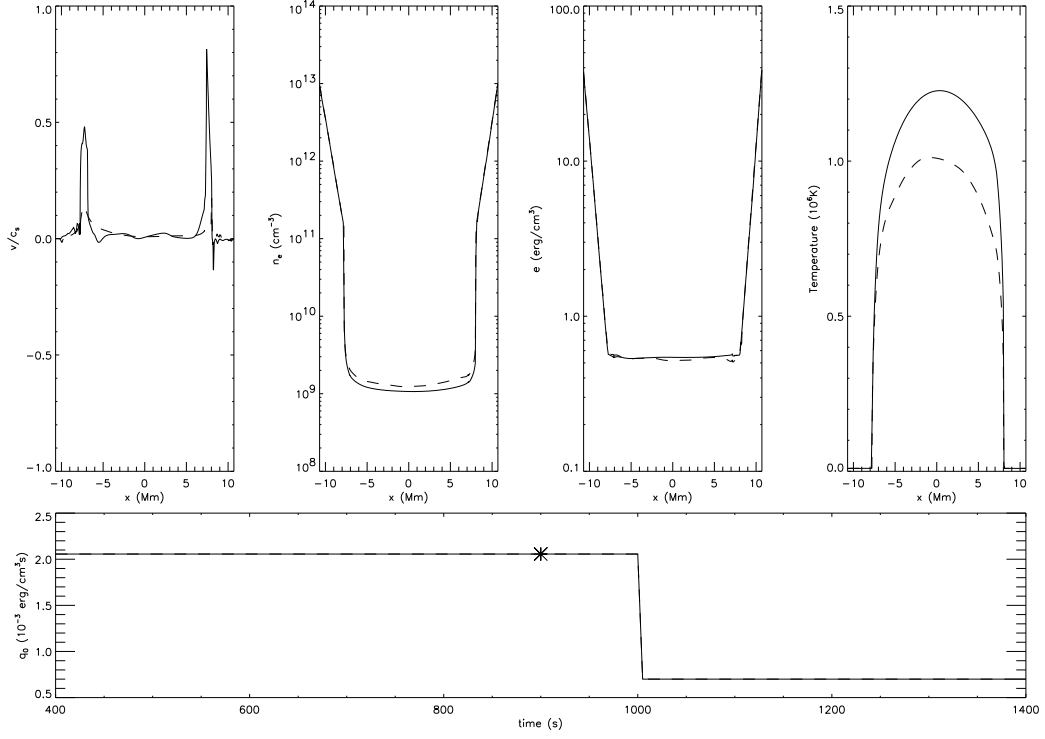


Figure 7: Frame 200, after 950 s of flare heating in a movie comparing the dynamics of XBP1 on two separate grids. Small differences in grid resolution lead to behavioral divergence.

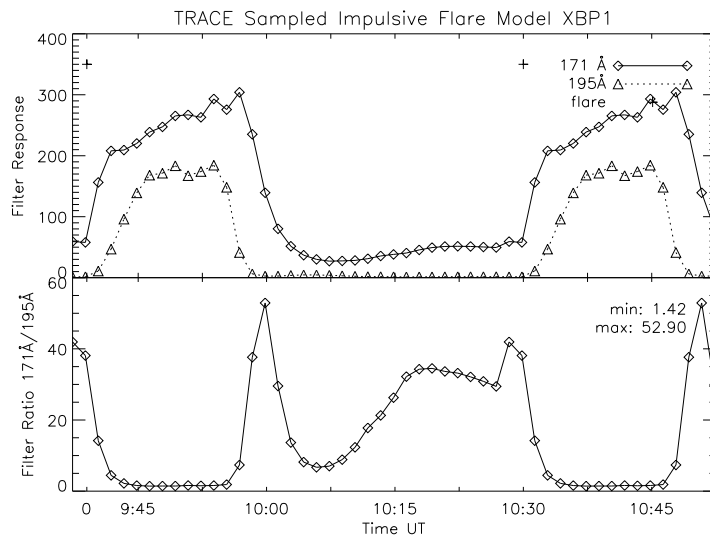


Figure 8: XBP1 model TRACE response for a single impulsive event. TRACE response generated by `ltrace.pro` code.

`ltrace.pro`. Sample light curves generated by this routine is in Figure 8

Another key routine is `nanoflare1.pro` which overlaps light curves at randomly generated times, rescaled to the average timing, and mimics an instrument response to a series of nano-flare events. Light curves generated by this routine are displayed in Figure 9.

References

- [1] E.H. Avrett, *New Models of the Chromosphere and Transition Region*, from *Mechanisms of Chromospheric and Coronal Heating*, Springer-Verlag, Berlin, 1991.¹
- [2] A.R. Choudhuri, *The Physics of Fluids and Plasma, an Introduction for Astrophysicists*, Cambridge University Press, 1998.
- [3] J.M. Fontenla, E.H. Avrett, R. Loeser, *Energy Balance in the Solar Transition Region. I. Hydrostatic Thermal Models With Ambipolar Diffusion*, *ApJ.*, **355**: 700, 1990.
- [4] J.D. Huba, *NRL Plasma Formulary*, Naval Research Laboratory, Revised 1998.
- [5] C.C. Kankelborg, D.W. Longcope, *Forward Modeling of the Coronal Response to Reconnection in an X-ray Bright Point*. *Solar Physics*, **190**: 59-77, 1999.
- [6] Lifshitz, Pitaevshkii, *Physical Kinetics*, Butterworth-Hinemann Ltd, 1999.
- [7] G. Peres, F. Reale. *The importance of plasma viscosity on X-ray line diagnostics of solar flares*. *Astronomy and Astrophysics*, **267**: 566-576, 1993.
- [8] D. Rabin, *Energy Balance in Coronal Funnels*, *ApJ.*, **383**: 407-419, 1991.

¹This paper is in a proceedings and hard to find, but C. Kankelborg has a hard copy.

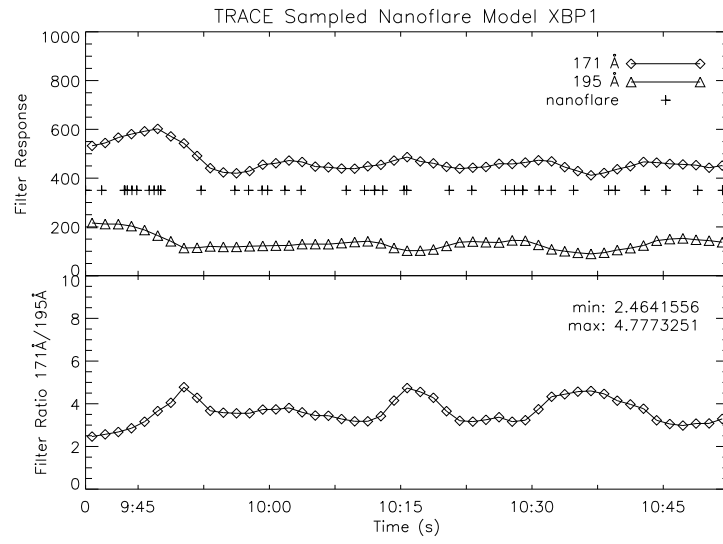


Figure 9: XBP1 model TRACE response to nanoflares. TRACE response generated by ltrace.pro code.

- [9] R. Rosner, W.H. Tucker, G.S. Vaiana *Dynamics of the Quiescent Solar Corona*. Astrophysical Journal, **22**: 643-665, 1978.
- [10] W. H. Press, S.A. Teukolsky, W. T. Vetterling, B. P. Flannery. *Numerical Recipes in C, The Art of Scientific Computing*. Second Edition. University of Cambridge, 1992.